Aust. J. Phys., 1990, **43**, 393–400

Imaging Semiconductors, Metals and Molecules with Scanning Tunneling Microscopy*

R. J. Wilson, S. Chiang and D. D. Chambliss

IBM Research Division, Almaden Research Center,
San Jose, CA 95120-6099, U.S.A.

Abstract

A brief review of applications of scanning tunneling microscopy (STM) to studies of clean and adsorbate covered surfaces is given. For metal-semiconductor systems, high resolution images provide insight into nucleation phenomena and atomic scale structure. For the metal on metal systems of Ag and Ni on Au(111) we report surprising new nucleation phenomena. Finally, we show that images of flat lying aromatic molecules can be obtained.

Scanning tunneling microscopy (STM) is a relatively new tool for studying the structure of surfaces (Binnig and Rohrer 1986). This technique has advanced considerably over the past few years and experience has indicated that, with due caution, it can be applied to many diverse systems. In this paper, we briefly review some of the results from our laboratory which relate to STM of semiconductors, metals, and absorbed molecules.

The STM we use resides in one chamber of an ultra high vacuum system with several different connected chambers for sample preparation and analysis (Chiang *et al.* 1988). The STM itself is comprised of a piezoelectric tripod, which carries a tungsten tip at small distance (~10 Å) from a single crystal surface of interest, a piezoelectric walker for bringing the sample to the tip, and vibration isolation mechanisms. The width of the vacuum gap between the sample and tip is maintained by applying a small bias voltage (~1 V) and maintaining a constant tunnel current by using feedback to control the tip position. The tip is slowly scanned parallel (x,y) to the surface and the voltage which is applied to the z piezo is recorded and converted into an image using various data processing algorithms. These images resemble topographic maps, but it is important to note that the tunnel current depends both on the local height of the surface and on the electronic density of states of both sample and tip. Additional complications arise if tip–sample interactions are sufficient to modify mechanical or electronic properties. These effects are important to an accurate interpretation of the data.

Some of the strengths and limitations of STM are apparent in work on the Ag/Si(111) system (Wilson and Chiang 1987*a*). Fig. 1 shows an image obtained on a Si(111) 7×7 crystal onto which 0·1 monolayer of Ag was evaporated at

* Paper presented at the Workshop on Interfaces in Molecular, Electron and Surface Physics, held at Fremantle, Australia, 4–7 February 1990.

0004-9506/90/040393$03.00

Fig. 1. A 150 Å×150 Å image of a low coverage Ag/Si(111) sample rendered with a false colour scale where black is low and yellow high. The upper left region is tiled with diamond shaped 7×7 cells. Ag nucleates at a step, lower right, and leads to a weakly corrugated honeycomb structure which extends out from the step edge.

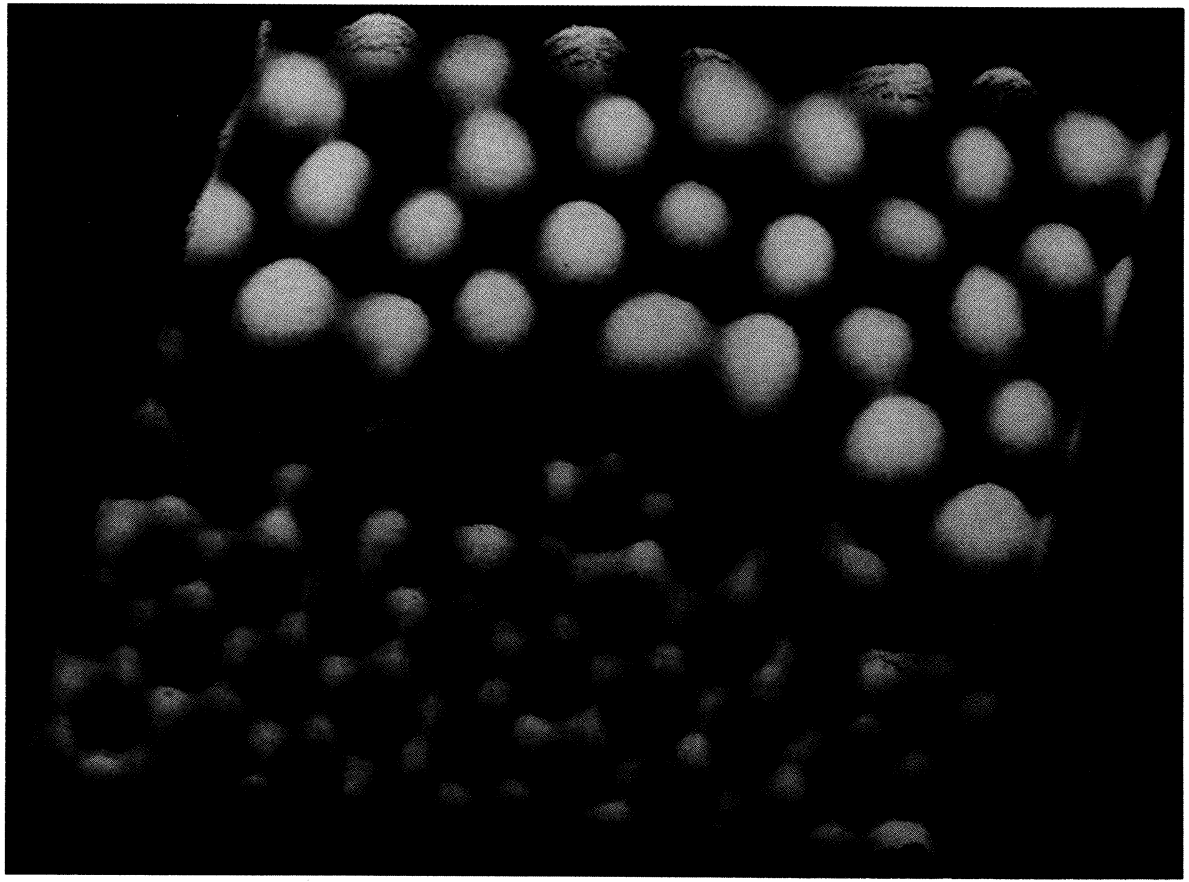

Fig. 2. A 90 Å×90 Å image of the transition region between clean and Ag coated Si(111). Data processing algorithms have been used to equalise the mean apparent heights of the two regions and to adjust the corrugation amplitudes so that they can be simultaneously visualised in a monochrome image.

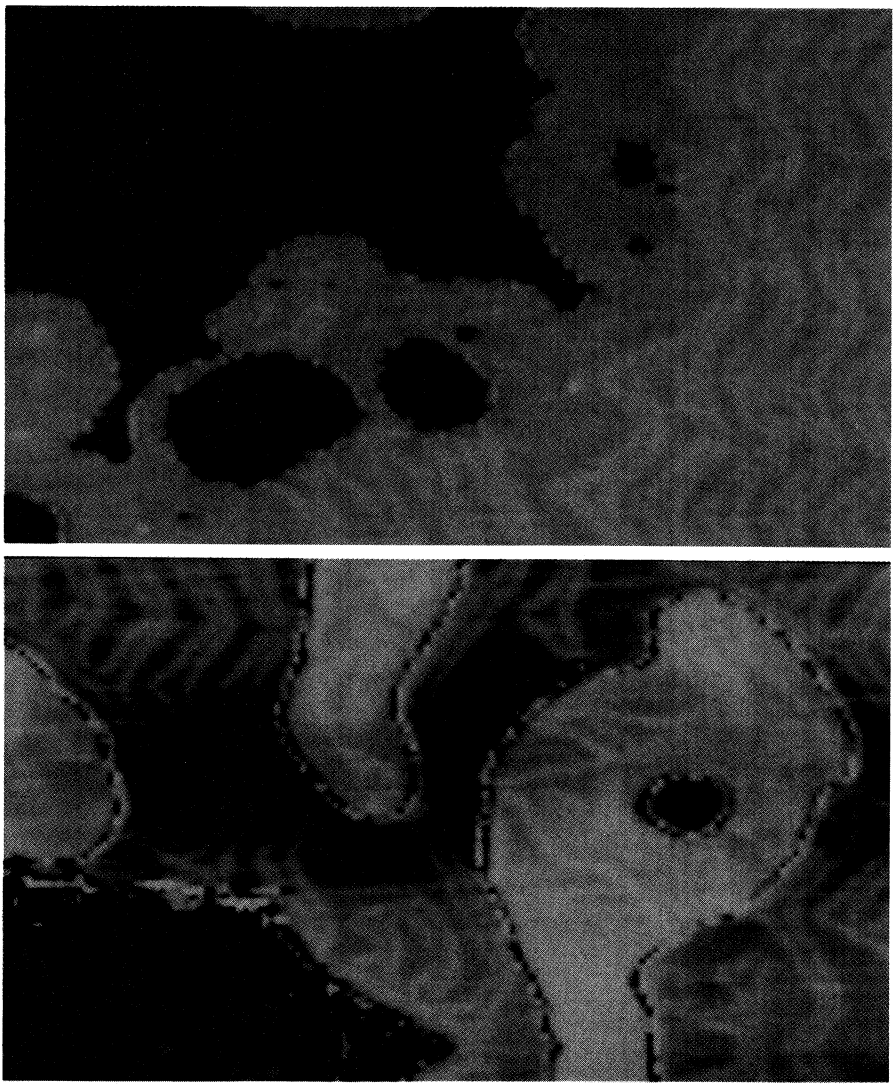

Fig. 3. Two 900 Å×900 Å images of Ag deposits on a Au(111) crystal. The upper image shows a pristine Au region, at the left, which is identified by the herringbone reconstruction pattern. Ag aggregates at the step edge to form the bright, unreconstructed rim along the upper terrace. The reconstruction on the lower terrace is highly distorted by strains associated with the Ag deposit. The corrugation associated with the reconstruction is small (and similar 0·15 Å) so that a constant is subtracted from points on the upper terrace to improve image contrast.

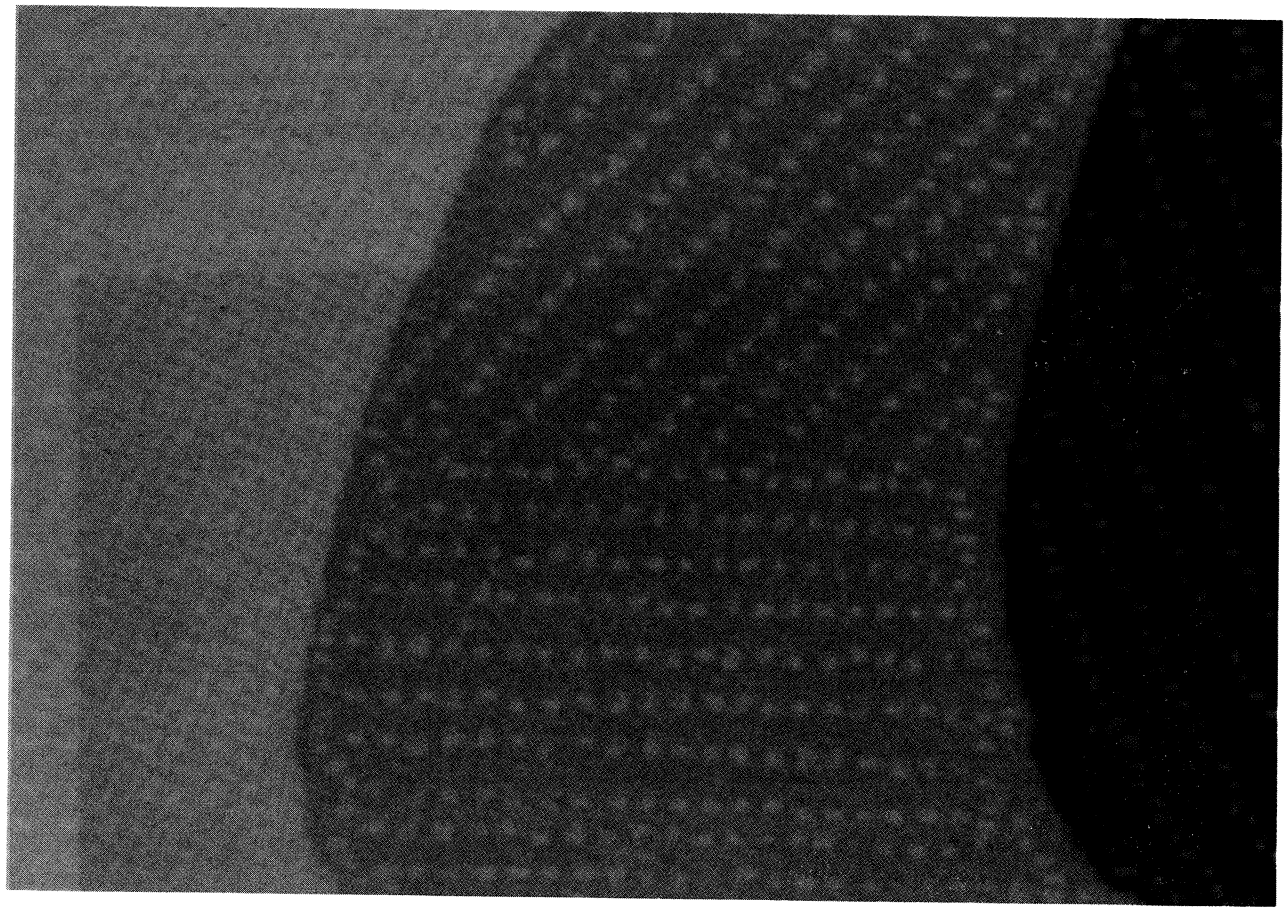

Fig. 4. A 2000 Å×2000 Å image of a low coverage Ni/Au(111) surface. Bright dots are Ni islands which nucleate at bends in the herringbone reconstruction of the clean Au(111). The herringbone dislocation array is not visible without the terrace height subtractions, used in Fig. 3, but manifests itself in the formation of three rotationally equivalent domains containing ordered arrays of Ni islands. Two such domains are apparent in this image.

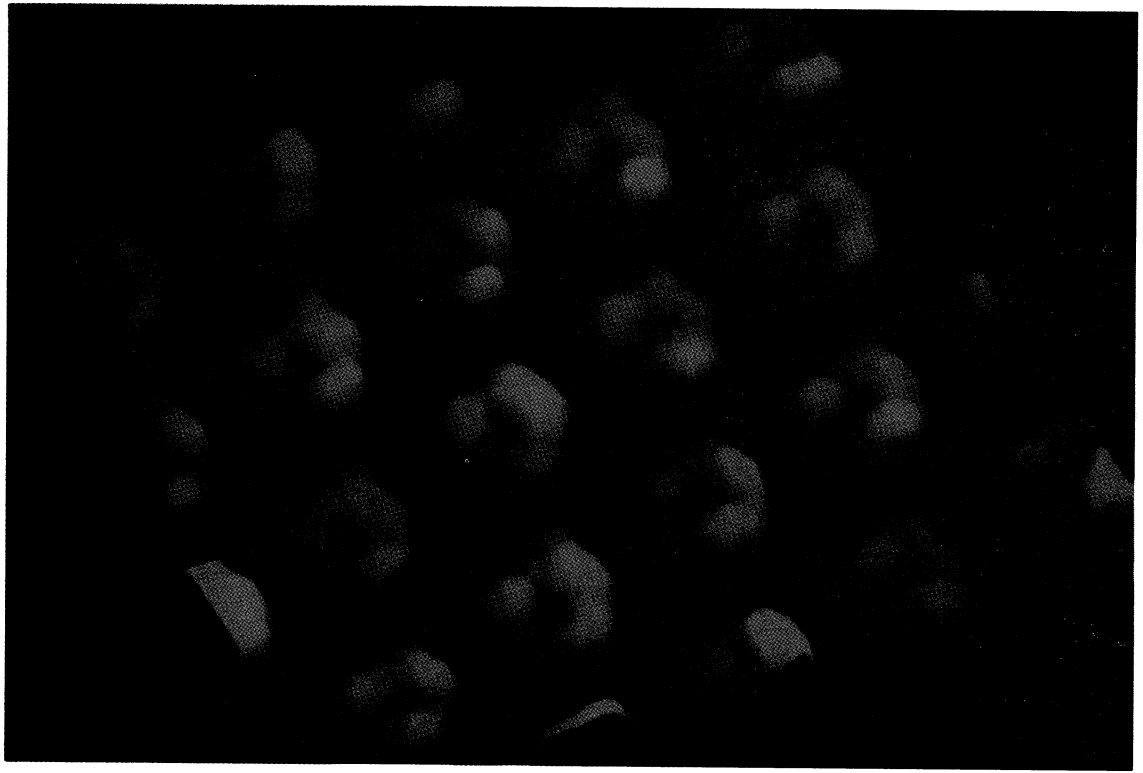

Fig. 5. A 60 Å×60 Å image of benzene and carbon monoxide molecules coadsorbed on a Rh(111) surface. Individual benzene molecules appear as distorted donut shaped structures. Carbon monoxide molecules are essentially invisible in this image. The contrast variation between these two molecules is not associated with molecular size, but rather is attributed to electronic structure effects.

600°C. Large, clean areas of the 7×7 reconstruction are found but near step edges a distinct $\sqrt{3}\times\sqrt{3}$ honeycomb structure appears on both upper and lower terraces. This honeycomb is a well known Ag/Si structure which had been previously studied by many techniques. The image shown here illustrates the strong potential of STM as a probe of nucleation and growth mechanisms. The boundary between clean Si and Ag coated Si can be studied at high magnification as shown in Fig. 2. This allows one to determine the positions of the protrusions relative to the underlying bulk lattice. Unfortunately, one cannot unambiguously identify these protrusions as Ag or Si atoms, or even as single atoms, from STM data without a thorough knowledge of electronic structure. In this particular case, different interpretations of essentially identical data have directly revealed this limitation (Wilson and Chiang 1987*a*; Van Loenen *et al.* 1987). Since the STM work, several new models have been put forward which are distinct from both of the models proposed on the basis of STM. Further work on other metal–semiconductor systems has revealed a wide diversity of behaviour (Wilson and Chiang 1987*b*; Wilson *et al.* 1988).

We have also been interested in metal surfaces and in metal on metal overlayer systems. For Au(111) we found that, under certain conditions, the corrugation of metal atoms (~0·1 Å) can be observed even in a close packed surface (Hallmark *et al.* 1987). This result was surprising in view of the delocalised nature of metallic conduction electrons. Again, similar results have been obtained by others but the interpretation remains controversial as it has been suggested that this corrugation actually results from strong interactions between the tip and surface which can lead to an amplification of the electronic corrugation (Woll *et al.* 1989). Wider scan images revealed stripe-like features which correspond to the $23\times\sqrt{3}$ reconstruction of the Au(111) surface (Chambliss *et al.* 1990). This reconstruction arises because the top layer of the Au(111) crystal contracts relative to the bulk leading to the formation of coherent arrays of partial dislocations. When the scan range was increased further, it was found for the first time that the Au(111) reconstruction actually forms into a herringbone superlattice with a very large unit cell (~140×70 Å^2). More recently, we have examined the growth of Ag and Ni overlayers at room temperature on this Au(111) surface (Batra and Ciraci 1988). Fig. 3 shows how Ag coalesces into irregular, unreconstructed deposits after diffusing across Au terraces to nucleate at step edges. Bare Au regions retain the herringbone reconstruction of the clean surface. Also evident are small Ag islands which show height variations similar to those of the Au(111) dislocations, but which are disordered. These images reveal the complex roles of strain and surface diffusion in epitaxial growth. For Ni the results are dramatically different as, at low coverages, monolayer Ni islands nucleate at each bend in the herringbone structure (see Fig. 4) resulting in ordered island arrays. As the Ni coverage is increased to ~0·5 ml, these islands begin to coalesce into Ni ribbons. This insight into the structure of metal overlayers suggests several methods for controlling the texture of surface layers. We hope to extend this work to alloy systems where one must expect significant complications due to intermixing and electronic structure.

STM studies of molecules are particularly difficult because molecules are typically weakly bound to surfaces and are not electrically conductive. Although

many of our attempts to image molecules have not succeeded, we have obtained good results for flat lying aromatics on non-noble metal surfaces. The first such study involved benzene, coadsorbed with CO, on a Rh(111) surface (see Fig. 5). Low resolution images clearly revealed the 3×3 array, expected from low energy electron diffraction measurements (Ohtani *et al.* 1988). At higher resolution, images showing ring-like structures, presumably distorted by interactions with the Rh surface, were obtained. Subsequently we examined Cu-phthalocyanine which can be adsorbed in multilayer quantities at room temperature. It was found that high resolution images could be obtained up to monolayer coverages on Cu(100), but that images of second layer molecules or of first layer molecules on Au(111) or Si(111) substrates were inadequate to identify molecular structure (Lippel *et al.* 1989). As in previous cases, both electronic structure effects and tip–surface interactions appear important. From this work, it appears that STM has promise for studies of relatively small molecules, where conductivity problems are not too important, and that the image quality is highly dependent on surface binding. Temperature remains an important, but largely unexplored, variable in these measurements.

This brief review is intended to whet the appetite rather than address STM with final authority. There are many problems and much controversy. But there is a beautiful simplicity to direct real imaging and we can just begin to appreciate the enormous variety of phenomena which can be viewed, and possibly controlled, on the microscopic scale.

Acknowledgment

This work was partially supported by the Office of Naval Research (N00014-89-C-0099).

References

Batra, I. P., and Ciraci, S. (1988). *J. Vac. Sci. Tech.* A **6**, 313.
Binnig, G., and Rohrer, H. (1986). *IBM J. Res. Dev.* **30**, 355.
Chambliss, D. D., Wilson, R. J., and Chiang, S. (1990). (to be published).
Chiang, S., Wilson, R. J., Gerber, Ch., and Hallmark, V. M. (1988). *J. Vac. Sci. Tech.* A **6**, 386.
Hallmark, V. M., Chiang, S., Rabolt, J. F., Swalen, J. D., and Wilson, R. J. (1987). *Phys. Rev. Lett.* **59**, 2879.
Lippel, P., Wilson, R. J., Miller, M. D., Woll, Ch., and Chiang, S. (1989). *Phys. Rev. Lett.* **62**, 171.
Ohtani, H., Wilson, R. J., Chiang, S., and Mate, C. M. (1988). *Phys. Rev. Lett.* **60**, 2398.
Van Loenen, E. J., Demuth, J. E., Tromp, R. M., and Hamers, R. J. (1987). *Phys. Rev. Lett.* **58**, 373.
Wilson, R. J., and Chiang, S. (1987*a*). *Phys. Rev. Lett.* **59**, 2329.
Wilson, R. J., and Chiang, S. (1987*b*). *Phys. Rev. Lett.* **58**, 2575.
Wilson, R. J., Chiang, S., and Salvan, F. (1988). *Phys. Rev.* B **38**, 12696.
Woll, Ch., Chiang, S., Wilson, R. J., and Lippel, P. (1989). *Phys. Rev.* B **39**, 7988.

Manuscript received 12 June, accepted 26 June 1990